Department of General Surgery[1], YouAn Hospital, Capital Medical University; Beijing Institute of Liver Disease[2]; Department of Clinical Pathology[3], YouAn Hospital, Capital Medical University, Beijing, China

Adenovirus vector-mediated herpes simplex virus-thymidine kinase gene/ganciclovir system exhibits anti-tumor effects in an orthotopic hepatocellular carcinoma model

Ruidong Zhu[1], Dexi Chen[2], Dongdong Lin[1], Fudong Lu[3], Jiming Yin[2], Ning Li[1]

Received November 3, 2013, accepted December 6, 2013

Ning Li, MD,PhD. Professor of Medicine, Department of General Surgery, YouAn Hospital, Capital Medical University, Beijing, 100069, China
liningbjah@163.com

Pharmazie 69: 547–552 (2014) *doi: 10.1691/ph.2014.3903*

Adenovirus vector-mediated herpes simplex virus-thymidine kinase/ganciclovir (ADV.tk/GCV) system is a promising approach for cancer gene therapy. This study aimed to investigate the anti-tumor efficacy and the underlying mechanisms of ADV.tk/GCV system in orthotopic hepatocellular carcinoma (HCC) model. A total of 132 female nude mice orthotopic HCC models were established and tumors were directly injected with ADV.tk (5.0×10^6 vector particles/kg) or saline solution, 24 h later the animals were intraperitoneally administrated by ganciclovir (30 mg/kg) or saline solution for 7 consecutive days. We observed that ADV.tk/GCV resulted in a significant regression of tumor growth and a significant prolongation of survival of the mice. At each given time point, the percentages of cleaved caspae-3, caspase-9 and TUNEL positive cells were significantly higher in the ADV.tk + GCV group than saline group ($P < 0.005$), while CD31 and VEGF staining were significantly less in ADV.tk + GCV group than in saline group ($P < 0.005$). In summary, ADV.tk/GCV system exhibits dramatic anti-tumor effects in orthotopic hepatocellular carcinoma model by promoting apoptosis and inhibiting angiogenesis, and is a promising treatment strategy for hepatic carcinoma.

1. Introduction

Hepatocellular carcinoma (HCC) is one of the most frequent and malignant diseases worldwide. HCC frequently develops from chronic hepatitis and/or cirrhosis, especially in sub-Saharan Africa and far eastern Asia, where hepatitis B and hepatitis C virus infection are endemic (de Martel et al. 2012; Ott et al. 2012). HCC became the second highest cause of cancer-related mortality (Jemal et al. 2011). Current standard treatment options, such as hepatic resection, liver transplantation and ablative therapies, can only be applied to a minority of patients because of the advanced disease at the time of diagnosis or the lack of suitable organ donors (Rampone et al. 2010; Cheng and Lv 2013). Therefore, the development of novel therapy strategies for HCC is of paramount importance (Zhang et al. 2012).

Suicide gene therapy, especially the herpes simplex virus thymidine kinase (HSV.tk)/ganciclovir (GCV) system, is a promising strategy for cancer therapy (Finzi et al. 2011). The expression of the *HSV.tk* gene in transduced cells can convert a nontoxic pro-drug, such as ganciclovir into a toxic nucleotide analog (ganciclovir triphosphate) that competes with triphosphate as a substrate for DNA polymerase. This inhibits both nuclear and mitochondria DNA synthesis, leading to cell death by apoptosis (Moolten 1986). A striking feature of this strategy is the so-called "bystander effect", whereby the adjacent non-transduced tumor cells also die, potentiating the anti-tumor efficacy (Hamel et al. 1996).

The efficacy of HSV.tk/GCV has been investigated in a number of tumor models (Kawashita et al. 2005; Hong et al. 2012). However, the exact pathway by which the ADV.tk/GCV system induces apoptosis in HCC *in vivo* remains elusive. Moreover, previous studies have preferentially used subcutaneous HCC models to evaluate the anti-tumor effects of the ADV.tk/GCV system. As subcutaneous tumor models do not possess tissue characteristics that could influence tumor growth and therapeutic effects, it is quite uncertain whether such data are applicable to the clinical situation (Bilbao et al. 2000; Palmer et al. 2006) Furthermore, HCC is one of the most vascular solid cancers characterized by neovascularization. Based on the bystander effects of the ADV.tk/GCV system, we hypothesize that the ADV.tk/GCV system can also inhibit angiogenesis and ultimately suppress HCC growth indirectly. For these reasons, we developed an orthotopic HCC mouse model to evaluate the anti-tumor efficacy and the underlying mechanisms of ADV.tk/GCV system.

2. Investigations and results

2.1. Adenovirus expression

Anti-adenovirus staining exhibited a marked signal in the transplanted tumors on day 3 after viral injection, and then the signal decreased (Fig. 1K). On day 23, only minute amounts of viruses were detected (Fig. 1E). As shown in Fig. 1A, a tumor nest was embraced by virus-infected cells, and a significant number of virus-infected cells were observed in adjacent necrotic tissue. The necrotic areas became gradually larger than that of the previous sacrificed animals with time prolonging (Fig. 1A-E). Although a small area of necrosis occurred, there was no positive staining in tumor tissues of saline control animals (Fig. 1F-J).

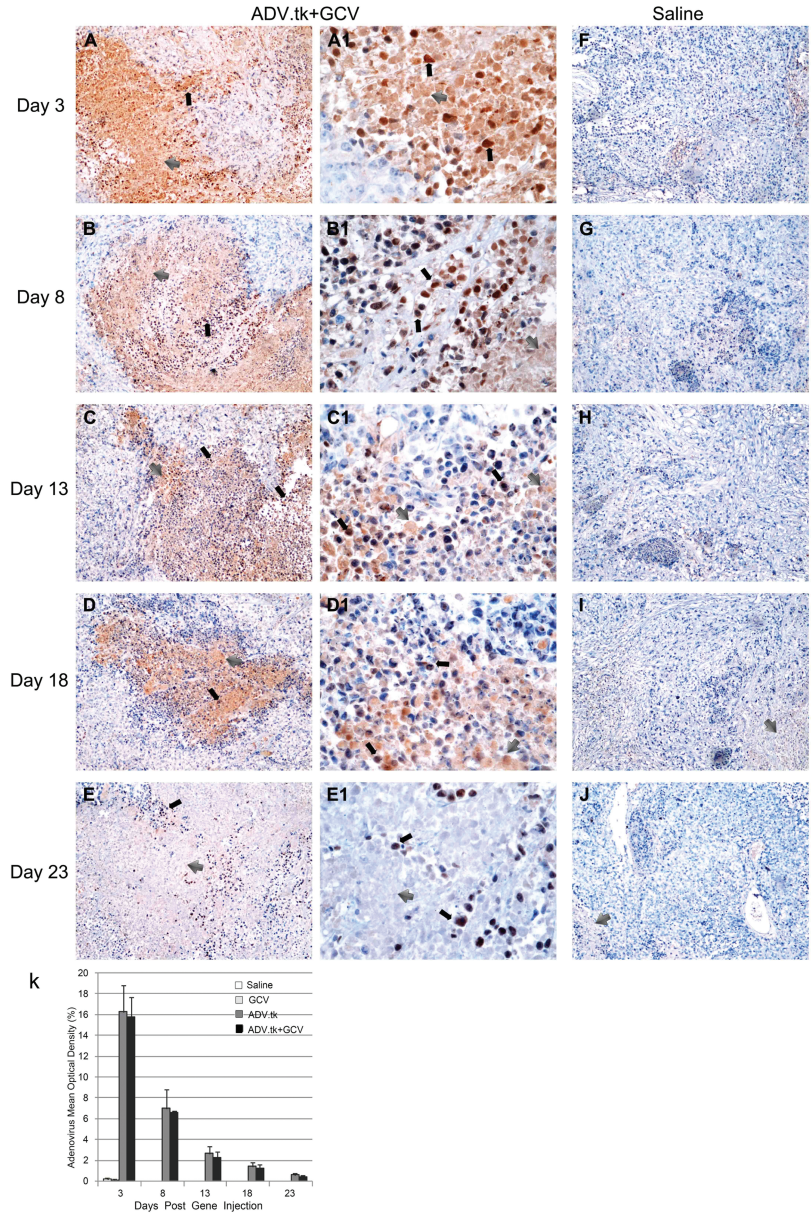

Fig. 1: Animals bearing orthotopic hepatic tumors were randomized in four groups: (I) saline solution alone; (II) saline + GCV; (III)ADV.tk + saline; (IV) ADV.tk + GCV. ADV.tk (5.0×10^6 vp/kg) or saline solution was injected intratumoraly and 24 h later animals were injected intraperitoneally with GCV (30 mg/kg) or saline for 7 days. Tumors were harvested on day 3, 8, 13, 18, and 23 after gene injection. Viral particles were detected by IHC staining using a mouse anti-adenovirus monoclonal antibody. A-E, A1-E1. Representative staining of ADV.tk + GCV treated tumors. F-J. Representative staining of saline treated tumors. Cells containing viral particles were stained deep brown (long arrow), and the necrotic cells were stained lighter (short arrow). K. Quantitation of adenovirus expression in the four groups. The duration of adenoviruses expression was about 23 days after gene injection. Magnification: 100 × (A-J), 400 × (A1-E1).

2.2. ADV.tk/GCV system inhibited tumor growth

After gene therapy, a clear tumor regression was observed in ADV.tk + GCV group on day 23 (Fig. 2A). At the end of the experiments, tumor sizes were reduced significantly in combined therapy group compared to saline group ($P = 0.026$). More specifically, on day 23, compared to saline group ($252.1 \pm 27.5\ mm^3$), GCV treatment reduced tumor growth by 15% ($214.4 \pm 49.8\ mm^3$), ADV.tk reduced tumor growth by 20% ($201.2 \pm 27.6\ mm^3$), the combination of ADV.tk + GCV treatment resulted in further tumor regression, with an inhibition rate of 52% ($126.5 \pm 34.4\ mm^3$). None of the mice exhibited severe toxicity during the experiments.

2.3. ADV.tk/GCV system prolonged the survival of tumor-bearing mice

A significant improvement in survival was observed in ADV.tk + GCV group (median survival time: 36 days) compared to that of the saline group (median survival time: 25 days) (Fig. 2B, $P = 0.046$). There was no significant difference in survival among ADV.tk (median survival time: 28 days), GCV (median survival time: 24 days) and saline treated animals. However, consecutive tumor regression was not achieved in ADV.tk + GCV group. At the end of the experiments, there was no significant difference in tumor mass among the four groups (Fig. 2C).

2.4. ADV.tk/GCV system promoted the apoptosis of tumor cells

To understand the mechanisms underlying the enhanced antitumor effects of the ADV.tk/GCV system, we assessed the apoptotic index in the tumor tissues. IHC analysis of cleaved caspase-9 showed that the staining was the strongest in combined therapy group (Fig. 3A-D, A1-D1). On day 13, the mean apoptotic index of caspase-9 was 0.64 in the combined

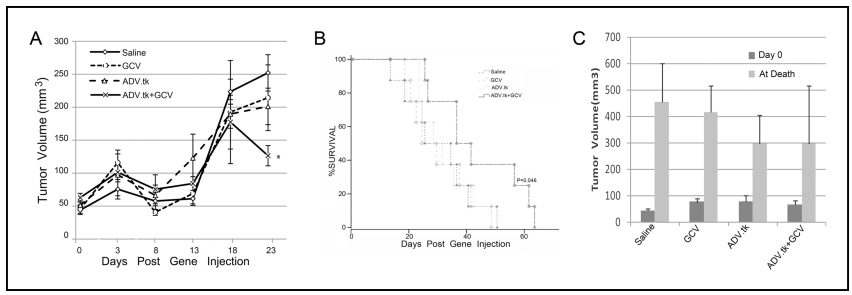

Fig. 2: ADV.tk/GCV system inhibits tumor growth. Animal models were grouped and treated as described in Fig. 1. A. Tumor volumes were measured at the indicated time points. Between day 13 and day 23, the tumors of the combined treatment group experienced a marked growth inhibition. On day 23, significant tumor regression occurred in ADV.tk + GCV group compared to saline group ($*p < 0.05$). B. Kaplan-Meier survival curve. ADV.tk + GCV group showed a significant prolongation of survival time compared to saline group ($P = 0.046$). C. Tumor sizes were calculated at the start of treatment (day 0) and on the day of animal death. Continuous tumor growth occurred and there was no significant difference in tumor volumes among the four groups.

treatment group, significantly higher than in the saline group (0.09) ($P < 0.001$, Fig. 3 M). Similarly, IHC analysis of cleaved caspase-3 showed that the staining was the strongest in combined therapy group (Fig. 3E-H, E1-H1). On day 23, the mean apoptotic index of caspase-3 was 0.30 in combined treatment group, significantly higher than in the saline group (0.09) ($P < 0.001$, Fig. 3N).

TUNEL staining further confirmed that the number of apoptotic cells was significantly higher in combined treatment group than in saline group (Fig. 3 I-L, I1-L1). Based on TUNEL staining, on day 13 and 23, the mean apoptotic index for combined treatment group were 0.35 and 0.63, while that of saline control group were 0.04 and 0.19, showing statistical significance, respectively ($P < 0.001$, Fig. 3O).

2.5. ADV.tk/GCV system inhibited tumor angiogenesis

To investigate the anti-angiogenic activity of the ADV.tk/GCV system, we detected the expressions of VEGF and CD31 in tumor tissues by IHC. Compared to the strong staining of VEGF in the saline group (IOD = 584.77 ± 18.66), we detected a weak VEGF staining in the ADV.tk + GCV group on day 18 (IOD = 8.17 ± 1.23, $P = 0.001$, Fig. 4A-D, A1-D1). At each indicated time point, VEGF expression in the combined therapy treated tumors was significantly lower than that of the saline treated tumors ($P < 0.005$, Fig. 4I). These data indicated that the ADV.tk/GCV system strongly inhibited VEGF secretion.

The significant anti-angiogenesis effect of the ADV.tk/GCV system was confirmed by IHC staining of CD31. On day 13, a significantly higher MVD was observed in saline treated tumors (165.10 ± 9.53) than in ADV.tk + GCV treated tumors (56.52 ± 5.89, $P < 0.001$, Fig. 4E-H). Moreover, the combination of ADV.tk transduction with GCV treatment caused a significant decrease in the number of tumor vessels at all given time points compared to the saline treated tumors ($P < 0.001$, Fig. 4J).

3. Discussion

Adenovirus vectors have been widely used for gene delivery in the experimental and clinical cancer gene therapy (Sung et al. 2001). However, serious obstacles in the use of adenovirus vectors remain, such as the induction of the host immune response and the relative short transgene expression which lasts approximately 3 weeks (Thomas et al. 2003). In the present study, the significant transgene expression was observed just after viral injection. The strong expression was transient and it decreased almost undetectable on day 23. However, the potential therapeutic effects lasted for a long time because even more dramatic apoptosis occurred on day 13 and 23. For suicide gene therapy, the destructive capacity which relies on the level of transgene expression is critical, while the duration of persistence is relatively less important (Ayala et al. 2006). Therefore, the first-generation adenoviral vectors are suitable for gene transfer in cancer gene therapy.

We observed a significant anti-tumor response in a nude mouse model using the combination of ADV.tk and GCV. Compared to the three control groups, the average tumor size of combined therapy group showed significant regression. The duration of tumor suppression was approximately three weeks, which coincided with the duration of adenovirus expression. In survival experiment, animals treated with ADV.tk + GCV demonstrated significant improvement in survival compared to that of the saline group. However, despite the prolonged survival, there was no significant difference in tumor volumes among the four groups at the end of this study. This suggests that after treatment was withdrawn, the tumors began to grow again. The main reason is that adenoviral vectors are incapable to deliver the functional gene to all HepG2 cells. Additional viral injections might offset this limitation.

We further investigated the anti-tumor mechanisms of the ADV.tk/GCV system. Our data indicate that suicide gene therapy can significantly suppress tumor angiogenesis and induce tumor cell apoptosis by intrinsic pathway. Apoptosis can occur *via* the extrinsic or the intrinsic pathway. The extrinsic pathway is triggered by ligation of death receptors on the cell surface, leading to caspase-8 activation, which then cleaves executioner caspase-3. The intrinsic pathway is mediated by Bcl-2 family proteins, which disrupt the mitochondria membrane and release Cytochrome C, and these factors would form an apoptosome to activate caspase-9, which then activates the downstream executioner caspase-3 (de Bruin and Medema 2008). The mechanism of HSV.tk/GCV induced apoptosis in HCC cells remains controversial. Some reports demonstrated that HSV.tk/GCV system induces apoptosis *via* a Bcl-2 controlled mitochondrial pathway (Fischer et al. 2005). However, other studies suggested that this system induces apoptosis by the activation of caspase-3, -8 and -9 (Shibata et al. 2003). To delineate the signal pathway of ADV.tk/GCV-induced apoptosis in HCC, the activities of caspase-3, and caspase-9 were analyzed by IHC and apoptosis was further confirmed by TUNEL assay. The results showed that the activities of caspase-3 and caspase-9 were significantly higher in the combined therapy group, accompanied by increased apoptotis, compared to other control groups. Therefore, we conclude that in our experimental setting, ADV.tk/GCV promotes tumor regression by significant augmentation of intrinsic pathway of apoptosis.

In the present study, we observed another important feature of ADV.tk gene therapy. The localized ADV.tk injection followed by systemic administration of ganciclovir resulted in a significant suppression in VEGF production and a dramatic reduction in MVD. In the hyper vascular tumor HCC, angiogenesis plays an important role in tumor growth, invasion, and metastasis (Zhu et al. 2011). VEGF is an endothelial cell-specific mitogen and a

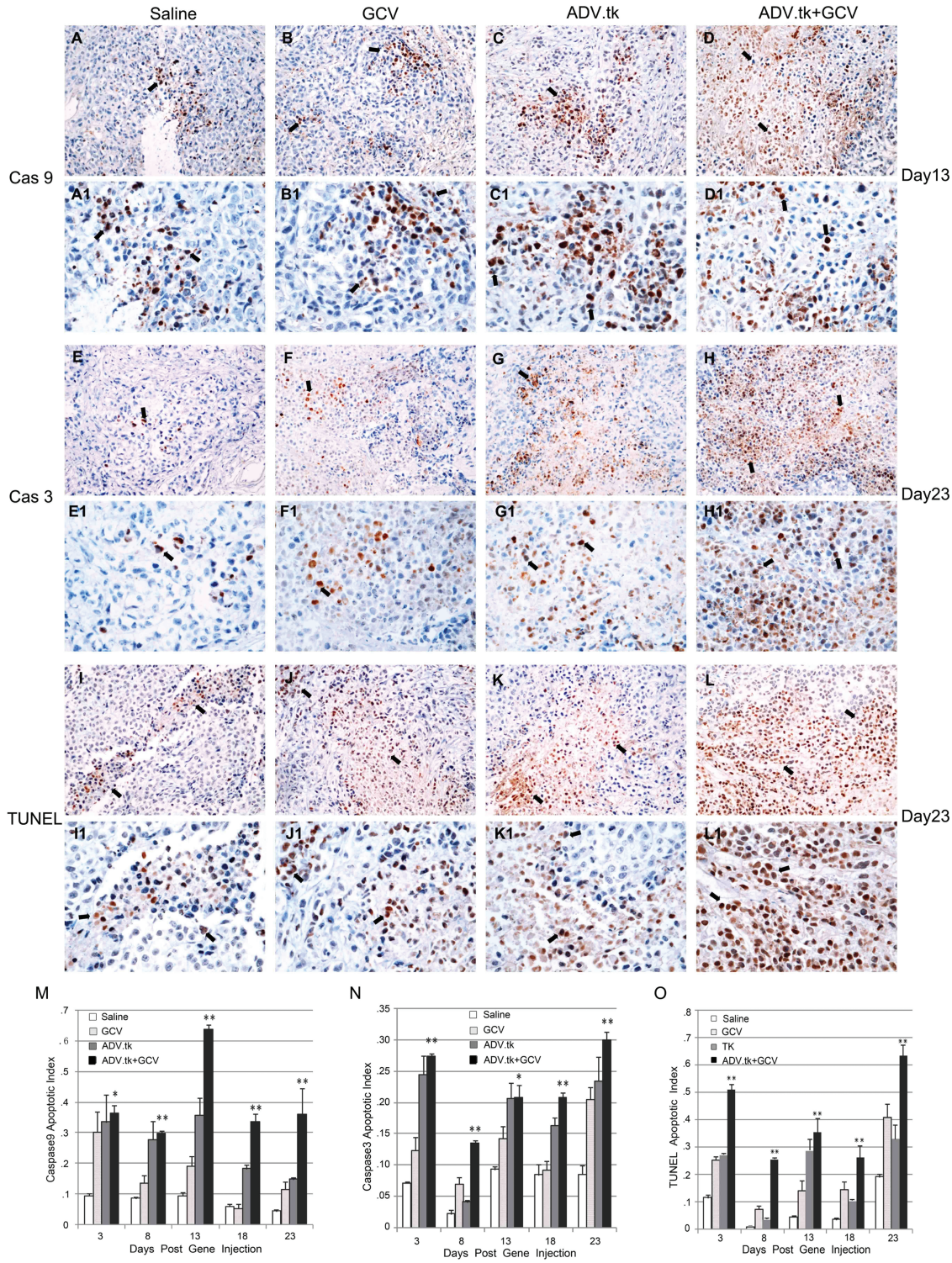

Fig. 3: ADV.tk/GCV system induces intrinsic apoptosis. Animal models were grouped and treated as described in Fig. 1, and tumor samples were processed by IHC or TUNEL staining. A-D and A1-D1. Representative staining of cleaved caspase-9 on day 13 after injection. E-H and E1-H1. Representative staining of cleaved caspase-3 on day 23 after injection. I-L and I1-L1. Representative staining of apoptotic cells by TUNEL technique on day 23 after injection. M. Quantization of caspase-9 apoptotic index of the four groups at each time point. N. Quantization of caspase-3 apoptotic index of the four groups at each time point. O. TUNEL apoptotic index of the four groups at each time point. Magnification: 200 × (A-L), 400 × (A1-L1). $^{*}P < 0.005$, $^{**}P < 0.001$, compared to saline group.

potent angiogenic factor that stimulates HCC angiogenesis and vascular permeability (Li et al. 2006). Therefore, ADV.tk/GCV system exerts additional anti-tumor effects partly by decreasing VEGF secretion, and reduces HCC angiogenesis.

In conclusion, in an orthotopic HepG2 carcinoma model we demonstrate that the therapeutic efficacy of the ADV.tk/GCV system is achieved by promoting the intrinsic pathway of apoptosis and inhibiting angiogenesis. Despite the limitation of the immune-incompetent model, our results support that the ADV.tk/GCV system can be part of a promising treatment strategy for hepatic carcinoma.

4. Experimental

4.1. Recombinant adenoviral vector

Recombinant replication defective adenoviral vectors (CE1A deleted) containing *HSV.tk* gene (ADV.tk) under the transcriptional control of the Rous sarcoma virus long terminal repeat was produced at Cancer Research Cen-

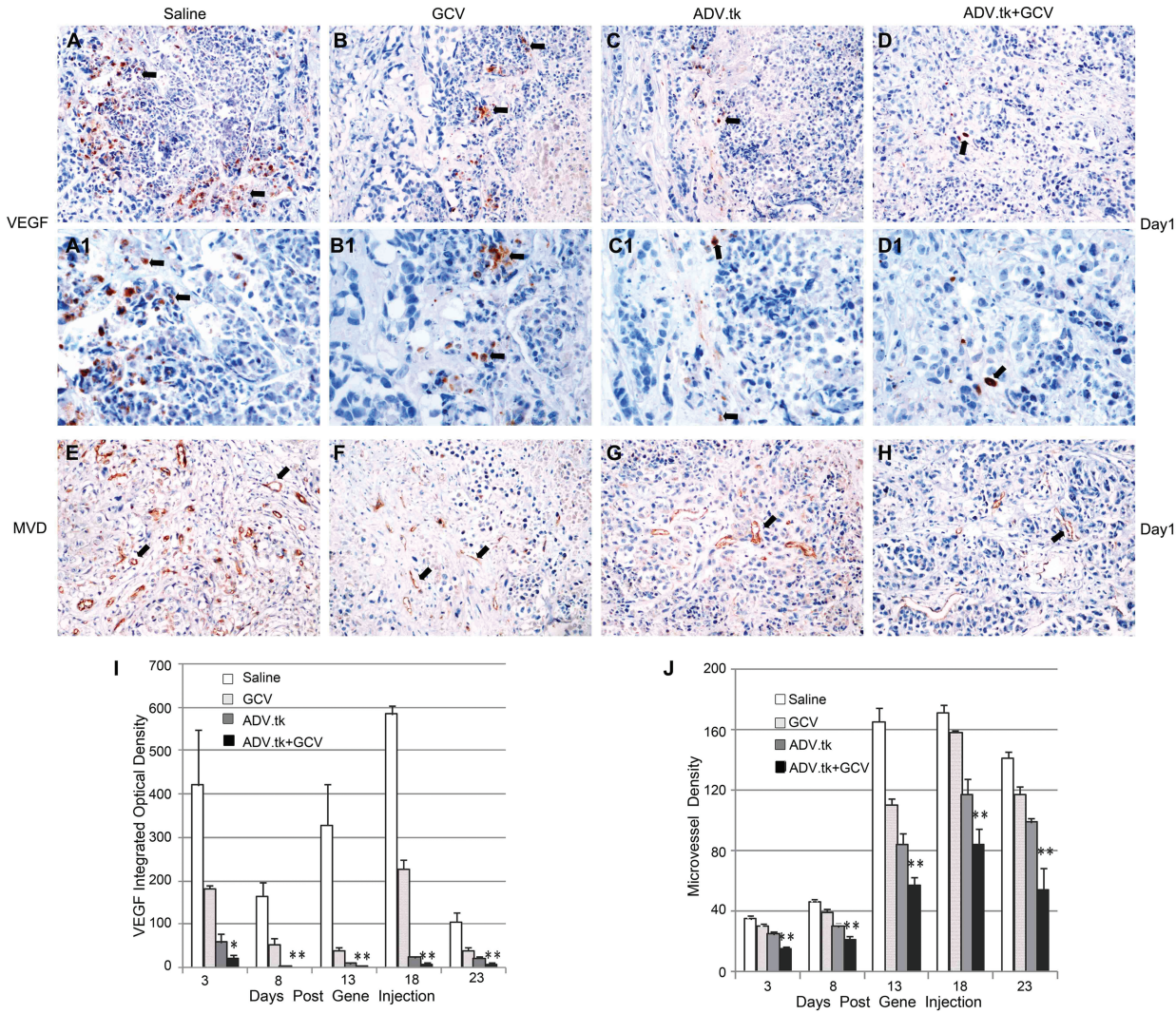

Fig. 4: ADV.tk/GCV system inhibits angiogenesis. Animal models and tumor samples were processed as described in Fig. 1 and VEGF expression and tumor microvessels were detected by IHC staining using rabbit anti-VEGF and -CD31 antibodies. A-D, A1-D1. Representative staining of VEGF in the four groups on day 18 after injection. E-H.. Representative staining of the microvessels in the four groups on day 13 after injection. I. Quantization of VEGF expression of the four groups. ADV.tk + GCV treatment significantly inhibited VEGF production compared to saline control group at each time point. J. Values of MVD of the four groups. ADV.tk + GCV treatment significantly decreased MVD in hepatic tumors compared to saline group at each time point. Magnification: 200 × (A-H),400 × (A1-D1). *$P < 0.005$, **$P < 0.001$, compared to saline group.

ter, Tongji Hospital, Tongji Medical College, following protocols described previously (Chang et al. 1995). Adenovirus was propagated in human embryonic kidney 293 cells (American Type Culture Collection), harvested 48 h after infection, and purified by the standard protocol of cesium chloride gradient centrifugation. Viral particles (vp/ml) were determined by spectrophotometric absorption and the purified adenoviruses were stored in phosphate-buffered saline (PBS) containing 10% glycerol at -80 °C, and diluted before the injection.

4.2. Cell culture

HepG2 cell line was obtained from the American Type Culture Collection (ATCC, Rockville, MD, USA). Cells were cultured in DMEM medium (Gibco, Gaithersburg, MD), supplemented with 10% fetal calf serum (Gibco, Gaithersburg, MD), 100 U/ml penicillin (Harbin Pharmaceutical Group) and 100 mg/ml streptomycin (North China Pharmaceutical Huasheng) in 5% CO_2 at 37 °C.

4.3. Animal models

Female BALB/c nude mice (4-week old) were obtained from Huafukang Bio-Technology Corporation (Beijing, China) and maintained under specific pathogen-free conditions. All animal experiments were approved by the Ethical Committee of the Tongji Medical College, Huazhong University of Science and Technology. Firstly, subcutaneous tumors were established by a single inoculation of 2×10^6 HepG2 cells into the dorsal flanks of nude mice. When the subcutaneous tumors had grown to 7–8 mm in diameter, the nude mice were euthanized, and then tumors were excised aseptically and cut into small pieces. Next, healthy mice were anesthetized by intraperitoneal injection of sodium pentobarbital (40 mg/kg) and their livers were surgically exposed and one tumor piece was implanted into the left lobe to allow transplanted hepatic tumor to grow (Gao et al. 2004). Three weeks later, an orthotopic HepG2 carcinoma model was established with tumor of 4–5 mm in diameter.

4.4. Single-therapy dose analysis

To define the optimal dose of ADV.tk for tumor regression *in vivo*, a preliminary dose response experiment was carried out. Viral doses ranged from 1.0×10^9 to 5.0×10^5 vp/kg were injected directly into the hepatic tumors followed by 7 days of GCV treatment at 30 mg/kg. A dose of 5.0×10^6 vp/kg achieved maximal tumor regression with minimal toxic reactions. This special viral dose was chosen for subsequent experiments.

4.5. Animal experiments

A total of 150 female BALB/c mice were implanted with tumor pieces as described above. Three weeks later, 147 mice (3 mice had died after the first surgery) were anesthetized and their livers were exposed for tumor measurements and drug administration. Total 132 orthotopic liver cancer models were successfully established and the tumor sizes were measured with caliper. Tumor volume was calculated by the formula $(a \times b^2)/2$, where a and b represented the largest and the smallest tumor diameters respectively (Zheng et al. 2009). Then, 50 µl ADV.tk (5.0×10^6 vp/kg) or 50 µl saline solution was injected directly into the hepatic tumors. The 132 mice were divided into four groups according to their treatment (n = 33): (I) saline

alone; (II) saline + GCV; (III) ADV.tk + saline; (IV) ADV.tk + GCV. Twenty-four hours later, the animals received 50 μl saline solution (group I and III) or 50 μl GCV (group II and IV, 30 mg/kg) intra-peritoneally, once a day, for 7 consecutive days.

For the survival experiment, eight mice were selected randomly from each group to evaluate the survival rate and calculate the final tumor volumes as soon as they died. The rest of the animals were sacrificed at 3, 8, 13, 18, 23 days (n = 5) respectively after injection. The mice which displayed signs of compromised health, such as lethargy, huddled posture, severe loss of weight, or vocalization, were euthanized. Hepatic tumors were harvested for tumor regression and IHC analysis.

4.6. IHC and TUNEL assay

The excised tumors were fixed in 10% buffered formalin, paraffin embedded and cut into 5 μm sections. IHC was performed using the PicTure^{TM} histological staining reagent Kit (PV-6000, Zhongshan Golden Bridge). Briefly, slides were deparaffinized in xylene and hydrated in ethanol. Endogenous peroxidase was blocked with 3%H_2O_2. The sections were then incubated overnight at 4 °C with primary antibodies: mouse anti-adenovirus monoclonal antibody (1:200;MAB8052, Chemicon), rabbit anti-human VEGF (1:200, ab9570, abcam) and CD31 (1:50, ab28364, abcam), rabbit anti-human cleaved caspase-3 (1:300, #9661, cell signaling Tech.) and cleaved caspase-9 (1:300, ab52299, abcam). After washing in phosphate buffered saline (PBS), the sections were incubated with anti-mouse or anti-rabbit antibody for 10 min at 37 °C. Immunoreaction products were visualized with diaminobenzidine (DAB) and then counterstained with hematoxylin. Negative controls were carried out by substitution of the primary antibodies with PBS.

TUNEL assay was performed using TUNEL kit (KGA7042, KeyGEN Biotech.) according to the manufacturer's instructions. Positive control samples were prepared by incubating with DNase I while negative controls were similarly processed by omitting TdT Enzyme.

Images were captured with a Nikon microscope (Nikon Eclipse 80i) and analyzed by Image-Pro Plus software (Image-Pro Plus version 6.0, Media Cybernetics). For each specimen, two sections were examined blindly by two investigators and the average of their scores was used. To quantify the intensity of adenovirus expression, three highest staining fields of each section were imaged at 100 × magnification, and expressed as mean optical density (MOD = IOD SUM/stained area SUM). To determine VEGF staining intensity, microvessel density and the quantity of apoptotic cells, six (VEGF, caspase-3,-9, TUNEL) or ten (CD31) areas in each section were imaged and measured, respectively. Ten areas of the highest vascular density area (hot spot) were selected for counting microvessel number under 200 × magnification. The average number of the vessels in the ten areas was calculated as MVD. The percentage of positive cells of cleaved caspase-3, caspase-9 and TUNEL staining were counted, respectively, as Apoptosis Index (AI). The intensity of VEGF expression was measured by Image-Pro Plus software and expressed as integrated optical density (IOD).

4.7. Statistical analysis

All data were expressed as mean ± S.E.M and statistical significance was set at $P < 0.05$. All P values were two-sided. Statistical analysis was performed with SPSS statistical package (SPSS version 17.0 for windows). Differences in tumor volume, relative increase of tumor volume, expression of adenovirus and VEGF, MVD, and apoptotic activity were compared using one-way analysis of variance (ANOVA). The Dunnett t test (doubled) was performed if the overall test was significant. The cumulative probability of survival was calculated by the Kaplan-Meier method and the significance of differences by the log-rank test.

Competing interests: The authors declare that they have no competing interests.

Acknowledgements: This study was supported by the Major National S&T Program of China (No.2012 ZX10002017-007). We thank Cancer Biology Research Center of Tongji Medical College, Huazhong University of Science and Technology for assistance. We gratefully acknowledge Jiliang Feng and Jun Lu (Beijing YouAn Hospital, Capital Medical University) for editing the manuscript.

References

Ayala G, Satoh T, Li R, Shalev M, Gdor Y, Aguilar-Cordova E, Frolov A, Wheeler TM, Miles BJ, Rauen K, Teh BS, Butler EB, Thompson TC, Kadmon D (2006) Biological response determinants in HSV-tk + ganciclovir gene therapy for prostate cancer. Mol Ther 13: 716–728.

Bilbao R, Gerolami R, Bralet MP, Qian C, Tran PL, Tennant B, Prieto J, Brechot C (2000) Transduction efficacy, antitumoral effect, and toxicity of adenovirus-mediated herpes simplex virus thymidine kinase/ganciclovir therapy of hepatocellular carcinoma: the woodchuck animal model. Cancer Gene Ther 7: 657–662.

Chang MW, Ohno T, Gordon D, Lu MM, Nabel GJ, Nabel EG, Leiden JM (1995) Adenovirus-mediated transfer of the herpes simplex virus thymidine kinase gene inhibits vascular smooth muscle cell proliferation and neointima formation following balloon angioplasty of the rat carotid artery. Mol Med 1: 172–181.

Cheng J-W, Lv Y. (2013). New progress of non-surgical treatments for hepatocellular carcinoma. Med Oncol 30: 1–9.

de Bruin EC, Medema JP (2008) Apoptosis and non-apoptotic deaths in cancer development and treatment response. Cancer Treat Rev 34: 737–749.

de Martel C, Ferlay J, Franceschi S, Vignat J, Bray F, Forman D, Plummer M (2012) Global burden of cancers attributable to infections in 2008: a review and synthetic analysis. Lancet Oncol 13: 607–615.

Finzi L, Kraemer A, Capron C, Noullet S, Goere D, Penna C, Nordlinger B, Legagneux J, Emile J-F, Malafosse R (2011) Improved retroviral suicide gene transfer in colon cancer cell lines after cell synchronization with methotrexate. J Exp Clin Cancer Res 30: 92.

Fischer U, Steffens S, Frank S, Rainov NG, Schulze-Osthoff K, Kramm CM (2005) Mechanisms of thymidine kinase/ganciclovir and cytosine deaminase/5-fluorocytosine suicide gene therapy-induced cell death in glioma cells. Oncogene 24: 1231–1243.

Gao YS, Chen XP, Li KY, Wu ZD (2004) Nude mice model of human hepatocellular carcinoma *via* orthotopic implantation of histologically intact tissue. World J Gastroenterol 10: 3107–3111.

Hamel W, Magnelli L, Chiarugi VP, Israel MA (1996) Herpes simplex virus thymidine kinase/ganciclovir-mediated apoptotic death of bystander cells. Cancer Res 56: 2697–2702.

Hong S, Zhang P, Zhang H, Jia L, Qu X, Yang Q, Rong F, Kong B (2012) Enforced effect of tk-MCP-1 fusion gene in ovarian cancer. J Exp Clin Cancer Res 31: 74.

Jemal A, Bray F, Center MM, Ferlay J, Ward E, Forman D (2011) Global cancer statistics. CA Cancer J Clin 61:69–90.

Kawashita Y, Ohtsuru A, Miki F, Kuroda H, Morishita M, Kaneda Y, Hatsushiba K, Kanematsu T, Yamashita S (2005) Eradication of hepatocellular carcinoma xenografts by radiolabelled, lipiodol-inducible gene therapy. Gene Ther 12: 1633–1639.

Li Q, Xu B, Fu L, Hao X (2006) Correlation of four vascular specific growth factors with carcinogenesis and portal vein tumor thrombus formation in human hepatocellular carcinoma. J Exp Clin Cancer Res 25: 405.

Moolten FL (1986) Tumor chemosensitivity conferred by inserted herpes thymidine kinase genes: paradigm for a prospective cancer control strategy. Cancer Res 46: 5276–5281.

Ott JJ, Stevens GA, Groeger J, Wiersma ST (2012) Global epidemiology of hepatitis B virus infection: new estimates of age-specific HBsAg seroprevalence and endemicity. Vaccine 30: 2212–2219.

Palmer DH, Young LS, Mautner V (2006) Cancer gene-therapy: clinical trials. Trends Biotechnol 24: 76–82.

Rampone B, Schiavone B, Confuorto G (2010) Current management of hepatocellular cancer. Curr Oncol Rep 12: 186–192.

Shibata MA, Horiguchi T, Morimoto J, Otsuki Y (2003) Massive apoptotic cell death in chemically induced rat urinary bladder carcinomas following in situ HSVtk electrogene transfer. J Gene Med 5: 219–231.

Sung MW, Yeh HC, Thung SN, Schwartz ME, Mandeli JP, Chen SH, Woo SLC (2001) Intratumoral adenovirus-mediated suicide gene transfer for hepatic metastases from colorectal adenocarcinoma: results of a phase I clinical trial. Mol Ther 4: 182–191.

Thomas CE, Ehrhardt A, Kay MA (2003) Progress and problems with the use of viral vectors for gene therapy. Nature Rev Genet 4: 346–358.

Zhang XJ, Ke LM, Yang J, Lin LW, Xue ES, Wang Y, Yu LY, Chen ZK (2012) Development, characterization and anti-tumor effect of a sequential sustained-release preparation containing ricin and cobra venom cytotoxin. Pharmazie 67: 618–621.

Zheng FQ, Xu Y, Yang RJ, Wu B, Tan XH, Qin YD, Zhang QW (2009) Combination effect of oncolytic adenovirus therapy and herpes simplex virus thymidine kinase/ganciclovir in hepatic carcinoma animal models. Acta Pharmacol Sin 30: 617–627.

Zhu AX, Duda DG, Sahani DV, Jain RK (2011) HCC and angiogenesis: possible targets and future directions. Nature Revi Clin Oncol 8: 292–301.